Counting Echoes: Application of a Complete Reciprocal-Space Description of NMR Spin Dynamics

RICHARD J. NELSON,[1] YAEL MAGUIRE,[2] DANIEL F. CAPUTO,[3] GABRIELA LEU,[3] YUN KANG,[1] MARCO PRAVIA,[3] DAVID TUCH,[3] YAAKOV S. WEINSTEIN,[1] DAVID G. CORY[3]

[1]*Department of Mechanical Engineering, Massachusetts Institute of Technology, Cambridge, Massachusetts* 02139
[2]*Media Arts and Sciences Laboratory, Massachusetts Institute of Technology, Cambridge, Massachusetts* 02139
[3]*Department of Nuclear Engineering, Massachusetts Institute of Technology, Cambridge, Massachusetts* 02139

ABSTRACT: A complete reciprocal-space formalism for describing the spatial aspects of nuclear magnetic resonance (NMR) spin dynamics in the presence of hard radiofrequency (RF) pulses and linear-refocusing inhomogeneities is reviewed. The formalism demonstrates how the magnetization in a sample can be decomposed into a linear combination of simple basis functions consisting of helical phase modulations in the transverse plane and sinusoidal amplitude modulations along the principal axis of symmetry. It is shown that plotting the evolution of the spatial Fourier variable for each basis function provides a simple way to compute both the number of echoes resulting from any multipulse experiment and when the echoes will form. The maximum number of echoes possible for a sequence of n hard RF pulses with 90°; flip angles and with arbitrary flip angles, both under the action of a time-invariant linear I_z Hamiltonian, is computed using this formalism. A simple criterion for the delay time necessary between pulses to observe the maximum number of echoes is presented. Experimental results are shown for pulse sequences of up to four pulses. Concepts Magn Reson 10: 331–341, 1998

KEY WORDS: spin echoes; k-space trajectories

Correspondence to: D. G. Cory.

Received March 4 1998; revised May 26, 1998; accepted May 26, 1998

Concepts in Magnetic Resonance, Vol. 10(6) 331–341 (1998)
 CCC 1043-7347/98/060331-11

INTRODUCTION

Spin echoes are indispensable elements for both imaging and spectroscopy experiments because of their ability to refocus selective interactions. Spin echoes were first discovered in 1950 by Hahn (*1*), and the theory of echo formation has been well established.

Until a few years ago, exact calculations to show the appearance times and amplitudes of spin echoes based on the theory of echo formation had been performed only under special circumstances. Carr and Purcell (*2*) and Woessner (*3*) directly integrated the Bloch equations (*4*) for sequences of up to four radiofrequency (RF) pulses. Ghose et al. (*5*), extending the spin-echo model developed by Banerjee et al. (*6*), correctly predicted the maximum number of echoes from a sequence of n hard pulses by invoking a physically nonexistent virtual stimulated echo mechanism, but did not indicate a simple way to determine when the echoes would appear. Using the fact that an echo forms when previously in-phase magnetization becomes refocused during a free induction period, Jensen (*7*) amplified the obscure spin-echo diagram originally attributable to Das and Saha (*8*) to predict the times and amplitudes of echo formation; similarly, Kaiser et al. (*9*) proposed a formalism for echo formation based on a partitioning of the magnetization vector into components of the same phase. These methods work adequately for periodic, symmetric pulse trains, but do not generalize easily to sequences with arbitrary flip angles, pulse phases, numbers of pulses, or different interpulse waiting times.

Recent work by Kim and Lee (*10*) corrected earlier work by Das and Roy (*11*) to predict the number of echoes produced by an arbitrary number of RF pulses, but their formalism relied on integrating the Bloch equations and deducing complex rules for magnetization pathways. Their work underscored the fact that as the number of RF pulses increases, the solution to the Bloch equations becomes appreciably more complex; furthermore, numerical evaluation of the expected induction signal is inflexible and provides little insight into the dynamics of echo formation. Finally, Hennig (*12*, *13*) developed a successful but sophisticated formalism that correctly predicts echo appearance times and amplitudes by defining substates that index the possible magnetization phase pathways induced by RF pulses. Although Hennig's extended phase graph formalism appears similar to the work presented in this article, it lacks the straightforward intuition and simpler mathematical description given here.

This work reviews a reciprocal-space formalism attributable to Sodickson and Cory (*14*, *15*) that completely describes the formation of spin echoes in an experiment of hard RF pulses and static field inhomogeneities. This approach provides a straightforward way to compute the appearance time and amplitude of all echoes due to linear effects by following trajectories in reciprocal space that contain the amplitude and phase information of each magnetization component in the sample. This method is then used to calculate the maximum number of echoes possible from a sequence of n hard RF pulses in the presence of a constant gradient field.

GENERALIZED *k*-SPACE FORMALISM

Consider the three Cartesian components of magnetization in a nuclear magnetic resonance (NMR) experiment. As is customary, the z axis is aligned with the external static field $\mathbf{B}_0$. During an experiment consisting of hard RF pulses, and refocusing inhomogeneities such as applied static magnetic field gradients, the magnetization vector field becomes in general a complicated function of position; this complex spatial dependence of the magnetization is called the magnetization grating. Decomposition of the grating into Fourier components of different spatial frequencies simplifies the description of the effects of RF fields and gradients on the magnetization grating. In this approach, known as the generalized k-space formalism, we examine the Fourier transform of the three components of magnetization, M_x, M_y, and M_z, under the action of magnetic field gradients and RF pulses.

Although this article specifically calculates the effects of static magnetic field gradients on the grating as found in an imaging experiment, this picture of the magnetization easily generalizes to a large class of spectroscopy experiments where the effects of other static refocusing inhomogeneities are the dominant interactions, such as static field inhomogeneities, background fields, or chemical shift differences (*14*, *15*). Indeed, since the Fourier transform is a linear mapping, this generalized k-space formalism accurately describes the magnetization in the sample under the action of any time-invariant linear I_z Hamiltonian.

Effect of Static Magnetic Field Gradient on Grating

When a magnetic field gradient is applied with a variation in magnetic field B_z, the components of the grating transverse to the z axis combine to form helical phase modulations (Fig. 1). If the gradient is applied such that the magnetic field varies along an arbitrary axis $\hat{u}$, the precession frequency of the magnetization in the transverse plane changes, or is phase modulated, according to

$$\gamma \frac{\partial B_z}{\partial u} u\, dt = u\, dk_u \qquad [1]$$

where γ is the gyromagnetic ratio, $(\partial B_z/\partial u)$ describes the magnetic field gradient, and k_u denotes the Fourier variable that contains the complete spatial dependence of the phase modulation. Referring to Fig. 1, k_u is a wavenumber that describes the pitch of the modulation. Considering the transverse magnetization variables M_x and M_y to be the real and imaginary parts of a single complex variable s, the phase modulation of the grating is proportional to

$$s(u, k_u) \propto e^{i(k_u u + \theta)} \qquad [2]$$

where θ is the constant phase offset for the entire sample, measured counterclockwise from the positive x axis in the x–y plane.

The effect of the gradient field is to change the wavenumber k_u of the transverse grating. Integrating Eq. [1] yields

$$\Delta k_u = \gamma \int \frac{\partial B_z}{\partial u}\, dt \qquad [3]$$

Hence, gradient evolution may be visualized as the tightening of the spatial helix in the direction of the gradient. If the magnetic field gradient is static, the effect of the field is to produce a modulation of k_u that is linear in time. Note that the gradient has no effect on θ.

Effect of an RF Pulse on Grating

In contrast to magnetic gradient effects, a hard RF pulse along a particular axis direction can be described as a rotation of the axis system around that axis. As a result, the new magnetization vector after an RF pulse is a linear combination of its components before the pulse. For example, consider an on-resonance, hard RF pulse α_ϕ, where α is the tip angle and ϕ is the phase of the pulse. If $\alpha = \pi/2$, a component of magnetization from the transverse plane modulated as $\sin(k_u u + \theta)$ is rotated into the z axis, creating a longitu-

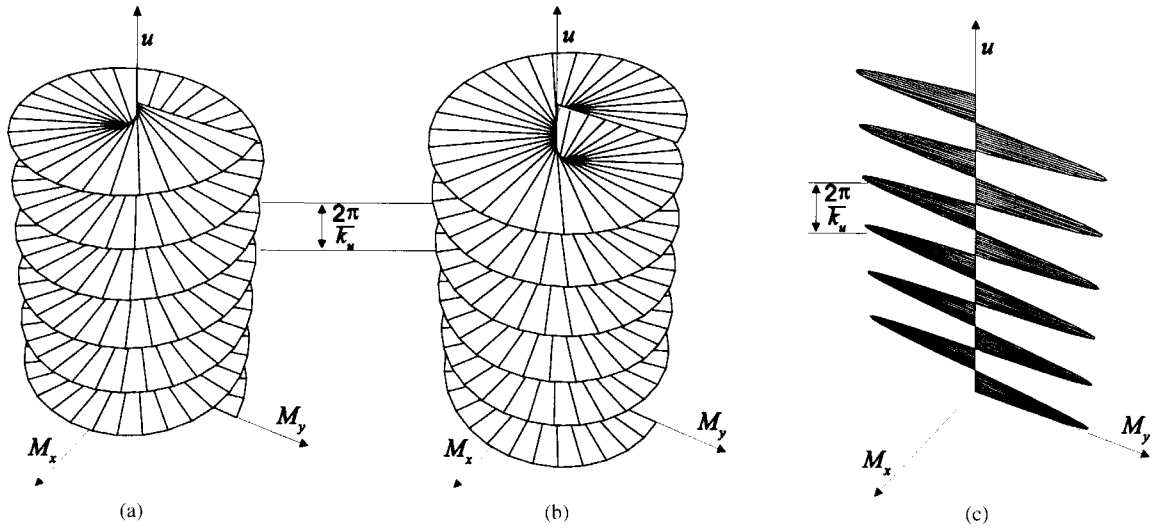

Figure 1 Magnetization grating caused by a linear magnetic field modulation along $\hat{u}$: (a) right-handed and (b) left-handed helical modulations of the magnetization, corresponding to phase-modulated grating components in the transverse plane; (c) a sinusoidal modulation of magnetization, corresponding to a longitudinal component.

dinal magnetization grating. In addition, if $\alpha = \pi$, then magnetization both along the z axis and along the axis transverse to both z and the pulse axis reverses their signs, or, equivalently, changes the sign of k_u on those axes.

Notice that if $\alpha < \pi/2$, only a fraction of the transverse magnetization is rotated into the z axis, but that the fraction depends only on α, not on k_u. The RF pulse causes mixing of longitudinal and transverse magnetization that may alter the overall phase θ, but has no effect on the absolute value of k_u.

How Magnetization Gratings Transform under RF Pulses

Note that any transverse magnetization can be written as the sum of right-handed and left-handed transverse helical gratings, phase modulated as in Eq. [2], over all values of k_u. In addition, any magnetization along the z axis can be written as the sum of longitudinal gratings, modulated as $\sin(k_u u + \theta)$, over all values of k_u [Fig. 1(c)]. Consequently, any spatial modulation of magnetization along $\hat{u}$ at any time t can be written as a linear combination of these three basis functions over all values of k_u:

$$\begin{aligned} \mathbf{g}_1(k_u, \theta) &= e^{i(k_u u + \theta)} \\ \mathbf{g}_2(k_u, \theta) &= e^{i(-k_u u + \theta)} \\ \mathbf{g}_z(k_u, \theta) &= \sin(k_u u + \theta) \end{aligned} \quad [4]$$

Since gradients affect only the transverse grating wavenumbers, and RF pulses mix components at constant k_u values, it is convenient to describe NMR experiments using this complete set of basis functions.

As previously noted, ideal, on-resonance RF pulses of the form α_ϕ cause mixing of the above basis functions that alters the amplitude and phase of the magnetization before the pulse. The derivation of the mixing amplitude and phase can be computed by considering the effect of the appropriate rotation matrices on the Cartesian components of magnetization, and then transforming to the basis set above; such computations have been carried out elsewhere (*12–15*) and can be summarized as:

$$\begin{bmatrix} \mathbf{g}_1(\theta) \\ \mathbf{g}_2(\theta) \\ \mathbf{g}_z(\theta) \end{bmatrix} \xrightarrow{\alpha_\phi} \begin{bmatrix} \cos^2\left(\frac{\alpha}{2}\right)\mathbf{g}_1(\theta) & +\sin^2\left(\frac{\alpha}{2}\right)\mathbf{g}_2(-\theta + 2\phi) & +\sin(\alpha)\mathbf{g}_z(\theta - \phi) \\ \sin^2\left(\frac{\alpha}{2}\right)\mathbf{g}_1(-\theta + 2\phi) & +\cos^2\left(\frac{\alpha}{2}\right)\mathbf{g}_2(\theta) & +\sin(\alpha)\mathbf{g}_z(-\theta + \phi + \pi) \\ \frac{1}{2}\sin(\alpha)\mathbf{g}_1(\theta + \phi + \pi) & +\frac{1}{2}\sin(\alpha)\mathbf{g}_2(-\theta + \phi) & +\cos(\alpha)\mathbf{g}_z(\theta) \end{bmatrix} \quad [5]$$

where it is understood that the k-value remains unchanged. These results can be modified further to include the effect of off-resonance pulses on the basis set, if necessary.

In summary, a sample at thermal equilibrium has all magnetization aligned with the external field B_0; an initial RF pulse at time t_0 creates some initial magnetization in the transverse plane; the gradient field creates modulations in the k-values of the magnetization grating; subsequent RF pulses cause mixing of the magnetization that can be described by the addition of grating components from the basis set, with their appropriate k-values. Thus, the magnetization grating is superimposed on the spin distribution, which for simplicity is assumed to be uniform and of infinite spatial extent. Since the detected signal is the transverse magnetization integrated over the sample volume, it is proportional to the grating amplitude at $k = 0$ (Fig. 2).

Tracking the evolution of the k-values for each magnetization grating present in the sample can easily be accomplished by plotting the k-space trajectories on a single graph. Note that the tra-

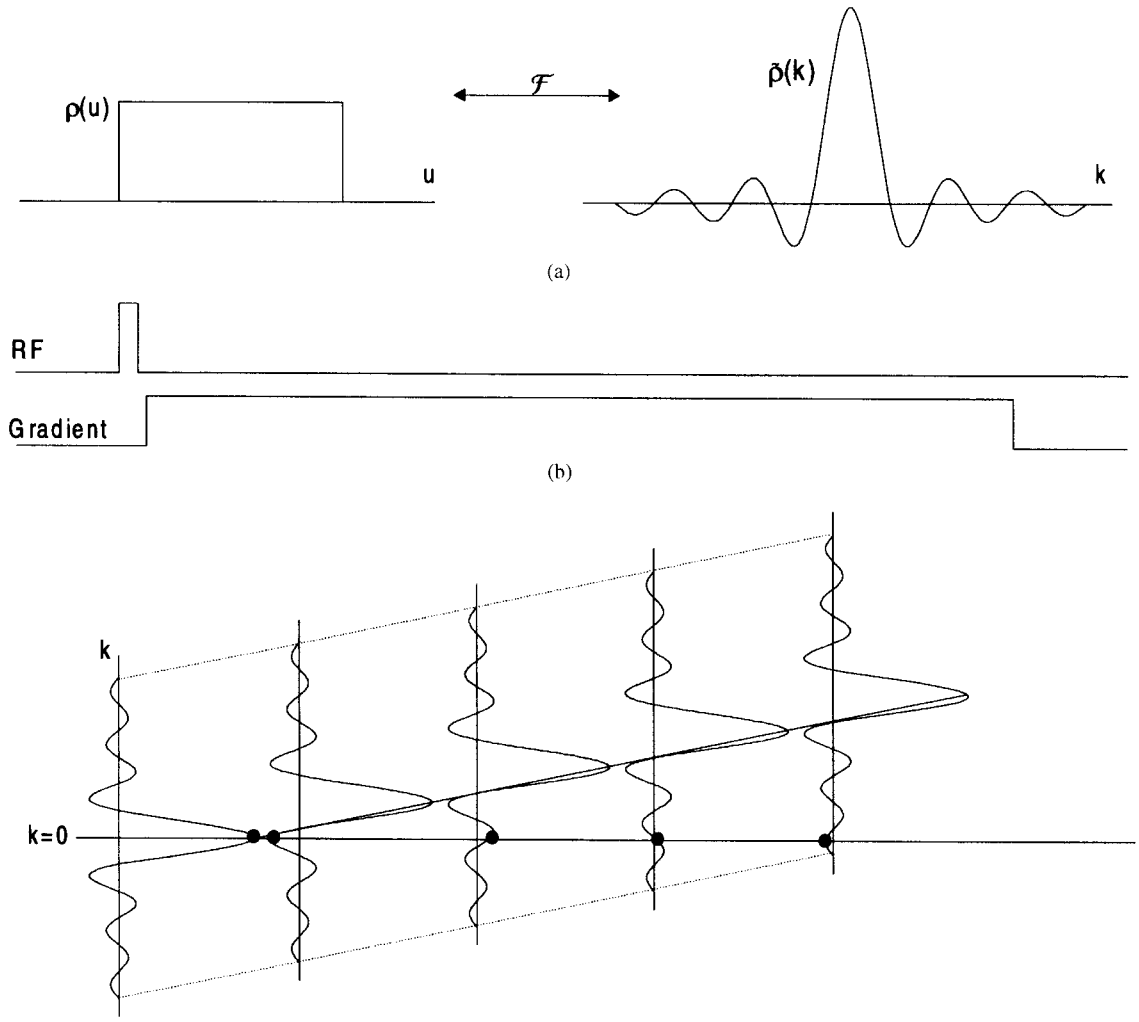

Figure 2 (a) Magnetization spin density, uniform along u, and its Fourier transform. (b) The evolution of a magnetization grating under the action of a time-invariant linear magnetic field gradient. The solid dots indicate the amplitude of the measured signal; the solid line shows the trajectory of the spatially uncorrelated k-value.

jectories for each of the components of the magnetization grating, described by the basis functions, completely describe the NMR experiment.

APPLICATION

The k-space description of the spin dynamics in an NMR experiment is not only complete in the sense that the formalism accounts for all the spatial information about the magnetization, but it also provides a straightforward way to compute the outcome of many NMR experiments. Consider the problem of determining the maximum possible number of echoes from a series of n hard RF pulses. Assume that the experiment is conducted in the presence of a constant B_0 gradient, whether a background gradient or intentionally applied, and assume enough time is allowed to elapse after each pulse to observe all echoes created by that pulse before the next pulse is applied. This maximum echo time delay between pulses can be trivially computed using the k-space picture, as shown later.

Calculation of Maximum Number of Echoes

This formerly complex problem may be accomplished in a straightforward manner using k-space trajectories. With the k-space description to track the spatial relations of the magnetization in the sample, determining the maximum number of

echoes produced by a series of n hard pulses reduces to counting the number of trajectories in k-space that cross the $k = 0$ axis. Since the rotation angle and rotation axis of the magnetization induced by each transverse RF pulse depend on the particular pulse sequence, the amplitude and phase of each trajectory will not be calculated, but rather only the existence of each possible trajectory and when the echo will occur. However, it should be noted that for any specific pulse-sequence experiment, computing the amplitude and phase of each trajectory simply amounts to a straightforward application of Eq. [5]. Finally, the amplitude of each echo can be calculated by including with the trajectory amplitude any attenuation, such as the effects of T_1 and T_2 relaxation, and diffusion.

Although the total number of echoes produced by a series of n pulses can be computed directly, it is instructive to solve this problem in three steps:

1. Determine the number of echoes that will result from the ith pulse in the series, assuming that only the first pulse rotates spatially uncorrelated magnetization into the transverse plane;
2. Determine the total number of echoes for all n pulses, with the same assumption as in step 1;
3. Determine the total number of echoes for all n pulses when each pulse rotates spatially uncorrelated magnetization into the transverse plane.

To label the possible trajectories, we will use the following nomenclature. Let a_i represent the number of $\mathbf{g}_1$ components (trajectories in k-space that have nonzero slope and $k > 0$), b_i the number of $\mathbf{g}_2$ components (trajectories with nonzero slope and $k < 0$), and p_i the number of $\mathbf{g}_z$ components (trajectories with zero slope and $k > 0$) of the grating immediately after the ith pulse (Fig. 3). It is useful to track these last trajectories, since they correspond to components of the magnetization that lie along the z axis after the ith pulse but will have a component of magnetization rotated into the transverse plane with the subsequent pulse. Without loss of generality, it is assumed that the gradient field has a positive value.

This procedure is applied to two cases: (a) the 90°; flip angle, where each pulse is a perfect $\pi/2$ pulse; and (b) the arbitrary flip angle, where each pulse has a flip angle not equal to an integer multiple of $\pi/2$ (for example, $\alpha < \pi/2$). This last case gives the maximum number of echoes possible from a sequence of n pulses.

The 90° Flip Angle Case.

1. Assuming only the first pulse rotates spatially uncorrelated magnetization into the transverse plane, a recursion relation between trajectories after the $(i - 1)$th pulse and the ith pulse can be computed by referring to Eq. [5] as follows:

- For a_i: All $a_i - 1$ trajectories have a component with slope and $k > 0$ after the ith pulse; in addition, all $b_i - 1$ trajectories will have a component with $k > 0$ after the ith pulse if enough time has elapsed since the $(i - 1)$th pulse so that they have all crossed the $k = 0$ line; finally, all $p_i - 1$ trajectories will be rotated into the transverse plane after the ith pulse.
- For b_i: The ith pulse causes all $a_i - 1$ trajectories to have a component with $k < 0$ after the pulse is applied; all $b_i - 1$ will also have a component with $k < 0$ after the ith pulse if enough time has elapsed to ensure that all $b_i - 1$ trajectories have crossed the $k = 0$ line; in addition, all $p_i - 1$ trajectories will be rotated into the transverse plane after the ith pulse.
- For p_i: All $a_i - 1$ and $b_i - 1$ trajectories will leave some magnetization along the z axis after the ith pulse.

The above relations may summarized as:

$$\begin{aligned} a_i &= a_{i-1} + b_{i-1} + p_{i-1} \\ b_i &= a_{i-1} + b_{i-1} + p_{i-1} \\ p_i &= a_{i-1} + b_{i-1} \end{aligned} \qquad [6]$$

Since each b_i gives rise to an echo when it crosses the $k = 0$ line, the simple recursion relation for the (maximum) number of echoes after the ith pulse is found from Eq. [6] as:

$$b_i = 2b_{i-1} + 2b_{i-2} \qquad [7]$$

or, by solving this difference equation:

$$b_{\alpha=\pi/2}(i) = \frac{1}{4\sqrt{3}}\left[(1 + \sqrt{3})^i - (1 - \sqrt{3})^i\right] \qquad [8]$$

for $i > 1$. (Note that $b_{\alpha=\pi/2}(1) = 0$, since

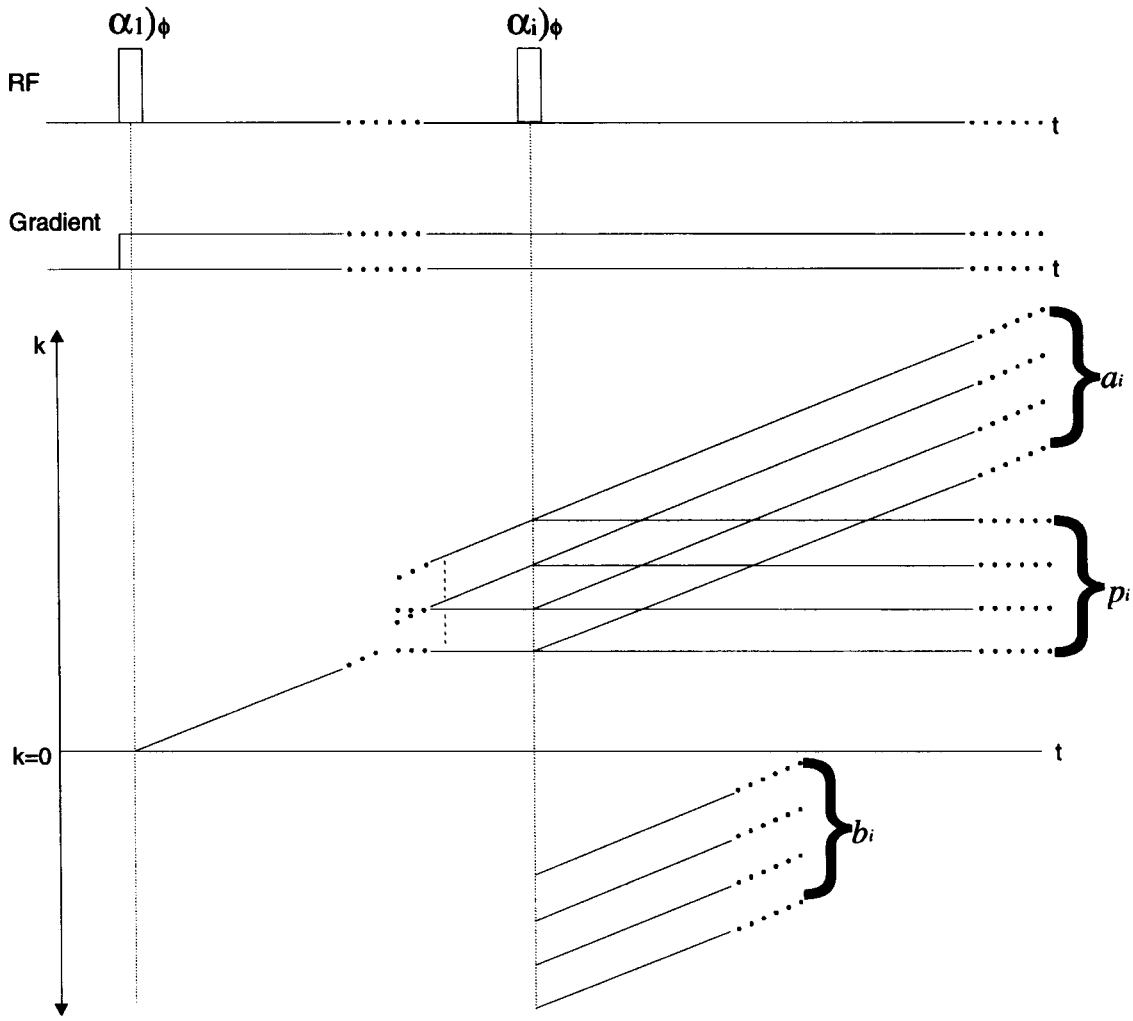

Figure 3 Counting trajectories: In general, pulse i produces a_i components of the grating described by basis functions of form $\mathbf{g}_1 b_i$ components described by basis functions $\mathbf{g}_2$, and p_i components stored along the z axis described by basis functions $\mathbf{g}_z$. An echo forms when one of the b_i lines crosses the $k = 0$ axis.

the first pulse gives rise to a single trajectory beginning at $k = 0$).

2. For a sequence of n pulses in which only the first pulse rotates uncorrelated magnetization into the transverse plane, the maximum number of echoes $N_{1,\alpha=\pi/2}$ is the sum of the maximum number of echoes from each pulse:

$$N_{1,\alpha=\pi/2}(n) = \sum_{i=1}^{n} b_{\alpha=\pi/2}(i) = \frac{1}{12}\left[(1+\sqrt{3})^{n+1} + (1-\sqrt{3})^{n+1}\right] - \frac{2}{3} \quad [9]$$

3. In addition to the trajectories accounted for by $N_1, \alpha = \pi/2$, each pulse also creates a new component of magnetization at $k = 0$ by rotating new magnetization from the z axis into the transverse plane. Hence, the maximum number of echoes $N_{\max,a=\pi/2}$ produced by a series of perfect 90° flip angle hard RF pulses is

$$N_{\max,\alpha=\pi/2}(n) = \sum_{i=1}^{n} N_{1,\alpha=\pi/2}(i) = \frac{1}{12\sqrt{3}}\left[(1+\sqrt{3})^{n+2} - (1-\sqrt{3})^{n+2}\right] - \frac{1}{3}(2n+1) \quad [10]$$

Note that in the more realistic case when each pulse rotates new magnetization into the transverse plane, the number of echoes produced by the ith pulse only is exactly equal to $N_{1,\alpha=\pi/2}$ and is precisely the solution that would have been found had this assumption been included in the recursion relations from the outset. Equations [9] and [10] are listed in Table 1 for values of n between 1 and 15.

Arbitrary Flip Angle Case.

1. As in the 90° flip angle case, first assume that only the first pulse begins a new k-space trajectory at $k = 0$ by rotating spatially uncorrelated magnetization into the transverse plane. By referring to Eq. [5], it is obvious that each RF pulse will cause each grating component to branch into a combination of all three basis functions. Equivalently, this case produces the same recursion relations as in the 90° flip angle case except that all p_i trajectories leave some magnetization along the z axis:

$$\begin{aligned} a_i &= a_{i-1} + b_{i-1} + p_{i-1} \\ b_i &= a_{i-1} + b_{i-1} + p_{i-1} \\ p_i &= a_{i-1} + b_{i-1} + p_{i-1} \end{aligned} \qquad [11]$$

As before, each b_i gives rise to an echo when it crosses the $k = 0$ line. In this case, the simple recursion relation for the (maximum) number of echoes after the ith pulse is

$$b_i = 3b_{i-1} \qquad [12]$$

or, by solving this difference equation

$$b(i) = 3^{i-2} \qquad [13]$$

for $i > 1$, where $b(1) = 0$ since the first pulse gives rise to a single trajectory beginning at $k = 0$.

2. For a sequence of n pulses in which only the first pulse rotates uncorrelated magnetization into the transverse plane, the maximum number of echoes N_1 is

$$N_1(n) = \tfrac{1}{2}(3^{n-1} - 1) \qquad [14]$$

3. Finally, in addition to the trajectories accounted for by N_1, each pulse also creates a new component of magnetization at $k = 0$ by rotating new magnetization from the z axis into the transverse plane. Hence, the maximum number of echoes N_{max} produced by a series of hard pulses is

$$N_{max}(n) = \tfrac{1}{4}(3^n - 2n - 1) \qquad [15]$$

This formula represents the absolute maximum number of echoes that can appear in an NMR experiment consisting of n hard RF pulses and linear refocusing inhomogeneities. Table 1 tabulates N_1 and N_{max} (Eqs. [14] and [15]) for pulse sequences of 1–15 pulses.

When the Last Echo Appears, and the Maximum Echo Time Delay

The k-space picture of the magnetization trajectories not only facilitates the above counting argument, but also clearly shows when each echo will appear. Of particular interest is when the last echo (typically called the direct spin echo of the first and last pulse) will appear after the ith pulse. Since the slopes of all the b_i trajectories are the same, the trajectory with the largest negative k-value after the ith pulse will cross the $k = 0$ line last. From Fig. 4(b), it is clear that this trajectory is the component of the original magnetization rotated into the transverse plane with the first pulse that is never stored along the z axis. Thus,

Table 1 Echoes from a Sequence of *n* Hard Pulses

	$\alpha = \pi/2$		$\alpha < \pi/2$	
n	$N_{1,\alpha=\pi/2}(n)$	$N_{max,\alpha=\pi/2}(n)$	$N_1(n)$	$N_{max}(n)$
1	0	0	0	0
2	1	1	1	1
3	4	5	4	5
4	12	17	13	18
5	34	51	40	58
6	94	145	121	179
7	258	403	364	543
8	706	1109	1093	1636
9	1930	3039	3280	4916
10	5274	8313	9841	14,757
11	14,410	22,723	29,524	44,281
12	39,370	62,093	88,573	132,854
13	107,562	169,655	265,720	398,574
14	293,866	463,521	797,161	1,195,735
15	802,858	1,266,379	2,391,484	3,587,219

$N_1(n)$ shows the maximum number of echoes after hard pulse n. $N_{max}(n)$ shows the maximum total number of echoes for a sequence of n hard pulses. The last column shows the maximum number of echoes that can be observed for a sequence of hard RF pulses in the presence of linear refocusing inhomogeneities.

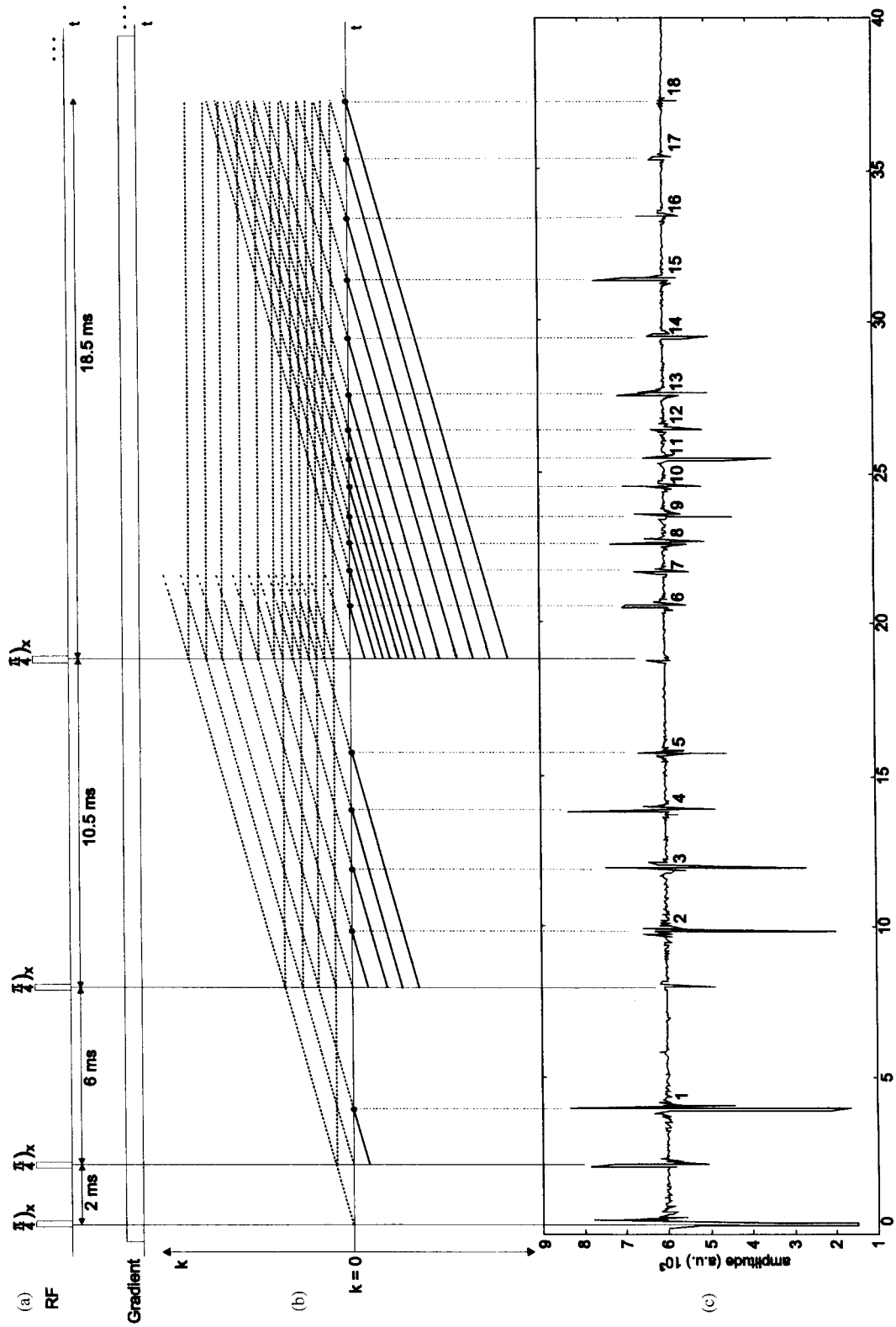

Figure 4 (a) A four-pulse sequence of hard RF pulses under the action of a constant linear I_z Hamiltonian, such as a magnetic field gradient. (b) The k-space picture for the sequence. The solid dots on the $k = 0$ line indicate the formation of an echo. (c) Experimental data in a sample of agrose gel. The 18 echoes, as predicted by Eq. [15], are clearly evident and occur as predicted by the k-space picture.

if the ith pulse occurs at time t_i after the first pulse, the last echo will appear at time $2t_i$ after the first pulse, regardless of the strength of the gradient.

To observe the maximum number of echoes from series of n hard pulses, it is useful to know the time to wait after a pulse before the next pulse is to be given. The first two pulses may be given at any time, since they do not lead to echo formation; thereafter, based on the above demonstration of when the last echo appears after the ith pulse, the delay between pulses must be

$$\Delta t_i = (t_i - t_{i-1}) > t_{i-1} = \sum_{j=2}^{i-1} \Delta t_j \qquad [16]$$

to observe all echoes. This is the maximum echo time delay criterion.

EXPERIMENT

Setup

To demonstrate the accuracy of Eq. [15], an NMR experiment was conducted using an applied B_0 gradient field and a sequence of four hard RF pulses. The sample consisted of an agrose gel, selected because of its good signal response and long relaxation times, run on a somewhat modified 3.0-T (122.19-MHz) Bruker AMX spectrometer. To allow all possible echoes to develop with large amplitudes, the four RF pulses were chosen with a flip angle of $\pi/4$. The delay times between pulses were chosen to be 2, 6, and 10.5 ms, respectively, in accordance with the maximum echo delay time criterion in Eq. [16]. The constant B_z gradient was chosen to allow good resolution of the echoes with acceptable signal losses. The entire sequence is illustrated in Fig. 4(a).

Results

Figure 4(c) shows the experimental results of the pulse sequence. As anticipated, the experiment produced the expected number of echoes: 18 total echoes for the four-pulse experiment. Figure 4(b) shows the k-space picture and accurately demonstrates the formation of each echo as indicated by a heavy mark when the trajectories cross the $k = 0$ line. Also note that the last RF pulse was given 18.5 ms after the first pulse, and that the last echo occurred precisely 18.5 ms after the last pulse, as predicted by the k-space picture.

CONCLUSIONS

In the absence of nonlinear effects, the maximum number of echoes from a train of n hard RF pulses in the presence of a refocusing inhomogeneity such as a weak magnetic field gradient is $N_{max}(n) = 1/4(3^n - 2n - 1)$. In addition, the last echo to be formed after a sequence of n hard pulses occurs after the last pulse an amount of time equal to the time after the first pulse that the nth pulse was given. These results demonstrate that the generalized k-space picture provides a complete picture of all echoes formed from time-invariant linear refocusing inhomogeneities.

Although the k-space picture reviewed here was used to investigate a simple gradient-pulse experiment, it has also been used to analyze imaging experiments, echo experiments, selective excitation sequences, and multiple quantum coherence gradient selection methods by including the effects of relaxation, flow, molecular diffusion, chemical shift, and spin–spin couplings (*9*, *10*). In most cases, use of the powerful k-space description of NMR spin dynamics simplifies the analysis over the use of numerical simulations of the Bloch equations or other, less intuitive methods.

REFERENCES

1. E. Hahn, "Spin Echoes," *Phys. Rev.*, **1950**, *80*, 580–594.
2. H. Carr and E. Purcell, "Effects of Diffusion on Free Precession in Nuclear Magnetic Resonance Experiments," *Phys. Rev.*, **1954**, *94*, 630–638.
3. D. Woessner, "Effects of Diffusion in Nuclear Magnetic Resonance Spin-Echo Experiments," *J. Chem. Phys.*, **1961**, *34*, 2057–2061.
4. F. Bloch, "Nuclear Induction," *Phys. Rev.*, **1946**, *70*, 460–474.
5. T. Ghose, S. Ghosh, and D. Roy, "Spin-Echoes with Any Number of Pulses," *Nuovo Cimento*, **1957**, *5*, 751–753.
6. B. Banerjee, S. Ghosh, and A. Saha, "A Nuclear Induction Spin-Echo Apparatus," *Indian J. Phys.*, **1957**, *4*, 221–226.
7. E. Jensen, "General Theory of Spin-Echoes for Any Combination of Any Number of Pulses," *Acta Polytech. Scand. Phys. Incl. Nucleon. Ser.*, **1960**, *7*, 1–20.
8. T. Das and A. Saha, "Mathematical Analysis of the Hahn Spin-Echo Experiment," *Phys. Rev.*, **1954**, *93*, 749–756.
9. R. Kaiser, E. Bartholdi, and R. Ernst, "Diffusion

and Field-Gradient Effects in NMR Fourier Spectroscopy," *J. Chem. Phys.*, **1974**, *60*, 2966–2979.
10. M. Kim and S. Lee, "Spin Echoes after Arbitrary *N* Pulses," *J. Magn. Reson.*, **1997**, *125*, 114–119.
11. T. Das and D. Roy, "Spin Echoes with Four Pulses —an Extension to *n* Pulses," *Phys. Rev.*, **1955**, *98*, 525–531.
12. J. Hennig, "Multiecho Imaging Sequences with Low Refocusing Flip Angles," *J. Magn. Reson.*, **1988**, *78*, 397–407.
13. J. Hennig, "Echoes—How to Generate, Recognize, Use or Avoid Them in MR-Imaging Sequences. Part I: Fundamental and Not So Fundamental Properties of Spin Echoes," *Concepts Magn. Reson.*, **1991**, *3*, 125–143.
14. A. Sodickson, "Spatial Aspects of Nuclear Magnetic Resonance Spectroscopy: Static and Radio Frequency Magnetic Field Gradients in Principle and Practice," 1997, Massachusetts Institute of Technology, Ph.D. thesis.
15. A. Sodickson and D. Cory, "A Generalized *k*-Space Formalism for Treating the Spatial Aspects of a Variety of NMR Experiments," *Progr. Nucl. Magn. Res. Spectrosc.* (submitted).

Richard J. Nelson, Yael Maguire, Daniel F. Caputo, Gabriela Leu, Marco Pravia, David Tuch, and **Yaakov S. Weinstein** are all graduate students in different departments at the Massachusetts Institute of Technology. Ranging in interests from mechanical to nuclear engineering and in academic standing from first- to final-year graduate student, they came together during the Fall semester of 1997 to study "Spatial Aspects of NMR Spectroscopy," a course taught by Proessor David G. Cory. This article matured from one of the required homework problems during the semester. The problem was aimed at demonstrating the benefits of keeping track of all spin magnetization in an experiment, rather than focusing on just the "paths of interest." Clearly, the approaches first introduced by Henning provide a very convenient framework for accomplishing this. From left to right: David Tuch, Gabriela Leu, Daniel F. Caputo, Marco Pravia, Yael Maguire, Yaakov S. Weinstein, and Richard J. Nelson. Not pictured: Yun Kang and David G. Cory.